J Membrane Biol (2009) 228:151–164
DOI 10.1007/s00232-009-9167-3

Novel Residues Lining the CFTR Chloride Channel Pore Identified by Functional Modification of Introduced Cysteines

Mohammad Fatehi · Paul Linsdell

Received: 2 February 2009 / Accepted: 24 March 2009 / Published online: 19 April 2009

Abstract Substituted cysteine accessibility mutagenesis (SCAM) has been used widely to identify pore-lining amino acid side chains in ion channel proteins. However, functional effects on permeation and gating can be difficult to separate, leading to uncertainty concerning the location of reactive cysteine side chains. We have combined SCAM with investigation of the charge-dependent effects of methanethiosulfonate (MTS) reagents on the functional permeation properties of cystic fibrosis transmembrane conductance regulator (CFTR) Cl^- channels. We find that cysteines substituted for seven out of 21 continuous amino acids in the eleventh and twelfth transmembrane (TM) regions can be modified by external application of positively charged [2-(trimethylammonium)ethyl] MTS bromide (MTSET) and negatively charged sodium [2-sulfonatoethyl] MTS (MTSES). Modification of these cysteines leads to changes in the open channel current–voltage relationship at both the macroscopic and single-channel current levels that reflect specific, charge-dependent effects on the rate of Cl^- permeation through the channel from the external solution. This approach therefore identifies amino acid side chains that lie within the permeation pathway. Cysteine mutagenesis of pore-lining residues also affects intrapore anion binding and anion selectivity, giving more information regarding the roles of these residues. Our results demonstrate a straightforward method of screening for pore-lining amino acids in ion channels. We suggest that TM11 contributes to the CFTR pore and that the extracellular loop between TMs 11 and 12 lies close to the outer mouth of the pore.

Keywords Chloride channel · Cystic fibrosis transmembrane conductance regulator · Ion channel pore · Permeation · Selectivity · Single channel · Site-directed mutagenesis · Substituted cysteine accessibility

M. Fatehi · P. Linsdell (✉)
Department of Physiology and Biophysics, Dalhousie University, 5850 College Street, Halifax, NS B3H 1X5, Canada
e-mail: paul.linsdell@dal.ca

Present Address:
M. Fatehi
Department of Biomedical Sciences, Atlantic Veterinary College, University of Prince Edward Island, 550 University Avenue, Charlottetown, PE C1A 4P3, Canada

Introduction

Cystic fibrosis is caused by mutations that lead to loss of function of the cystic fibrosis transmembrane conductance regulator (CFTR) Cl^- channel, a member of the ATP-binding cassette (ABC) family of membrane transport proteins (Gadsby et al. 2006). Direct structural information on CFTR is available only at low resolution but appears to show a monomeric transmembrane (TM) protein with a central pore lined by multiple membrane-spanning α-helices (Rosenberg et al., 2004). This overall structure is in common with bacterial ABC proteins for which higher-resolution structures are available (Dawson and Locher 2006; Linton 2007) and is reflected in current homology-based molecular models of CFTR (Mornon et al. 2008; Serohijos et al. 2008). Information about the structure of the TM pore in CFTR and the mechanism of Cl^- permeation has come from investigation of the functional consequences of site-directed mutagenesis within the 12 TM regions (Kidd, Kogan and Bear 2004; Linsdell 2006) (Fig. 1). The importance of these regions in forming the pore has been demonstrated by mutagenesis-induced changes in channel

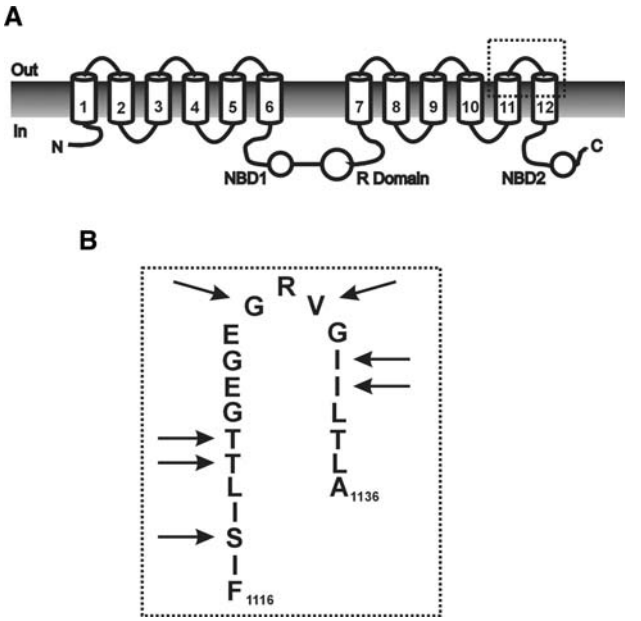

Fig. 1 Location of amino acid residues mutated in the present study. **a** Overall topology of CFTR, comprising 12 TMs (arranged in two groups of six), two cytoplasmic nucleotide binding domains (NBDs) and the cytoplasmic R domain. *Boxed region* represents the region mutated in the present study, comprising extracellular parts of TMs 11 and 12 and the short extracellular loop joining these two TMs. **b** Primary amino acid sequence of the region boxed in (**a**), identifying the 21 residues mutated individually to cysteines, from F1116 (in TM11) to A1136 (in TM12). *Arrows* indicate residues that were functionally modified by MTS reagents in our experiments

properties such as single-channel conductance (Sheppard et al. 1993; McDonough et al. 1994; Linsdell et al. 1998; Smith et al. 2001; Ge et al. 2004), interactions with permeant (Gupta et al. 2001; Ge et al. 2004) and blocking ions (McDonough et al. 1994; Linsdell 2005; St. Aubin et al. 2007; Zhou et al. 2007), anion selectivity (Linsdell et al. 2000; McCarty and Zhang 2001; Ge et al. 2004), the shape of the current–voltage (*I–V*) relationship (Smith et al. 2001; Ge et al. 2004; St. Aubin and Linsdell 2006) and substituted cysteine accessibility mutagenesis (SCAM) (Akabas et al. 1994; Cheung and Akabas 1996; Akabas 1998; Beck et al. 2008).

The SCAM approach (Karlin and Akabas 1998) has been very widely used to identify amino acid side chains which line the pore of ion channels. The principle behind this approach is that the covalent reaction between water-soluble substances (usually methanethiosulfonate [MTS] reagents) and solvent-accessible cysteine side chains will cause a change in channel function. While this is a very powerful approach, there are well-known caveats to its use as a screen for pore-lining amino acid side chains. For example, covalent modification of side chains at any water-accessible site, such as an exposed surface or water-filled crevice, may result in changes in channel function that could lead to false positives. Usually, a change in macroscopic current amplitude resulting from MTS modification is monitored, which could result from changes in channel open probability, channel conductance or both; these do not necessarily reflect directly changes in pore function. On the other hand, more traditional structure–function analysis of putative pore-forming amino acid residues can identify non-pore-lining residues that influence channel properties indirectly.

In the present work we have sought to combine the strengths of SCAM and the functional analysis of Cl^- permeation to identify new residues lining the CFTR channel pore. We investigated the charge-dependent effects of MTS modification of cysteine residues on Cl^- permeation. Previously, we showed that covalent modification of cysteine residues introduced at different sites in TM6 by charged MTS reagents added to the extracellular solution altered the shape of the *I–V* relationship, due to altered electrostatic interactions between extracellular Cl^- ions and the pore (Fatehi and Linsdell 2008). A similar approach had previously been used to modify the surface charge present at the outer (Smith et al. 2001) and inner (St. Aubin and Linsdell 2006) mouths of the pore. Here, we used the functional modification of introduced cysteines to scan the external parts of TMs 11 and 12 and the short extracellular loop that joins these two TMs (Fig. 1). While it has been predicted that these TMs would contribute to the pore (McCarty 2000; Kidd et al. 2004), functional evidence supporting their involvement in determining the permeation properties of the pore is limited and inconclusive (McDonough et al. 1994; Vankeerberghen et al. 1998; Zhang et al. 2000; Gupta et al. 2001; McCarty and Zhang 2001) and there has been no systematic investigation of the relative roles of different residues in this part of the CFTR protein. As well as demonstrating the utility of the functional modification of introduced cysteines as a simple screen for novel pore-lining amino acids, our results identify TM11 and the extracellular loop between TMs 11 and 12 as contributing to the CFTR channel pore.

Methods

Experiments were carried out on baby hamster kidney cells transfected with wild-type or mutant forms of human CFTR. Most experiments used cells that had been stably transfected with the pNUT-CFTR vector and selected using methotrexate (Chang et al. 1998). In a small number of cases, cells transiently transfected with the pIRES2-EGFP-CFTR vector (Gong et al. 2002) were used. No differences were noted between experiments carried out on stably or transiently transfected cells. In both cases, mutagenesis was carried out using the QuikChange system (Stratagene,

La Jolla, CA) as described previously (Gong et al. 2002) and verified by DNA sequencing. Macroscopic and single-channel patch-clamp recordings were made from inside–out membrane patches excised from these cells, as described in detail previously (Gong et al. 2002; Ge et al. 2004; St. Aubin and Linsdell 2006). Following patch excision and recording of background currents, CFTR channels were activated by exposure to protein kinase A catalytic subunit (PKA) plus MgATP (1 mM) in the cytoplasmic solution. Single-channel currents were recorded after weak PKA stimulation (1–5 nM), whereas macroscopic currents were recorded after maximal PKA stimulation (~20 nM) and subsequent treatment with sodium pyrophosphate (PPi, 2 mM) to maximize channel open probability. As a result, both macroscopic and single-channel currents reflect the open channel *I–V* relationship (Linsdell and Gong 2002; Gong and Linsdell 2003a; Fatehi et al. 2007). Both intracellular (bath) and extracellular (pipette) solutions contained (mM) 150 NaCl, 2 $MgCl_2$ and 10 *N*-tris(hydroxymethyl)methyl-2-aminoethanesulfonate (TES). To estimate channel SCN^- permeability (Fig. 11), NaCl in the intracellular solution was replaced by 150 mM NaSCN. In these experiments, membrane voltages were corrected for liquid junction potentials calculated using pCLAMP9 software (Molecular Devices, Sunnyvale, CA). All experimental solutions were adjusted to pH 7.4 using NaOH.

Channels were exposed to extracellular cysteine-reactive MTS reagents by inclusion of these substances in the pipette solution during inside–out patch recordings. This was necessary because many sites in the pore are not modified by negatively charged sodium [2-sulfonatoethyl] methanethiosulfonate (MTSES) prior to channel activation (Fatehi and Linsdell 2008). It is assumed that channels were fully modified during the experiment, and indeed, no time-dependent changes in apparent modification were noticed. As a result of exposure to MTS reagents during seal formation and channel activation, patches do not have their own pre-MTS controls and channel currents are compared between different patches recorded under different modification conditions (Fatehi and Linsdell 2008; Zhou et al. 2008). Both MTSES and the positively charged [2-(trimethylammonium)ethyl] methanethiosulfonate bromide (MTSET) were initially prepared as high-concentration stock solutions and stored frozen at −20°C as small-volume aliquots until the time of use, when they were added to the pipette solution at a final concentration of 5 mM.

All chemicals were obtained from Sigma-Aldrich (Oakville, Canada) except PKA (Promega, Madison, WI) and MTSES and MTSET (Toronto Research Chemicals, North York, Canada).

Current traces were filtered at 100 Hz using an 8-pole Bessel filter, digitized at 250 Hz (for single-channel currents) or 1 kHz (for macroscopic currents) and analyzed using pCLAMP9 software. Macroscopic *I–V* relationships were constructed using depolarizing voltage-ramp protocols, with a rate of change of voltage of 50–100 m*V* s^{-1} (Linsdell and Hanrahan 1996, 1998). Background (leak) currents recorded before addition of PKA and ATP were subtracted digitally, leaving uncontaminated CFTR currents (Linsdell and Hanrahan 1998; Gong and Linsdell 2003a). Rectification of the *I–V* relationship was quantified as the *rectification ratio*, the slope conductance at –50 m*V* as a fraction of that at +50 m*V* (Gong and Linsdell 2003b; Linsdell 2005). Relative *I–V* shape under different conditions was compared graphically by plotting the current from each patch as a fraction of that recorded at –80 m*V* (I_{REL}) (Fatehi and Linsdell 2008; Zhou et al. 2008). The macroscopic current reversal potential (V_{rev}) was estimated by fitting a polynomial function to the leak-subtracted *I–V* relationship and used to calculate the permeability of SCN^- relative to that of Cl^- (P_{SCN}/P_{Cl}) according to the following equation:

$$V_{rev} = (RT/F)\ \ln\left[\left(P_{SCN}[SCN]_i + P_{Cl}[Cl]_i\right)/\left(P_{Cl}[Cl]_o\right)\right]$$

where $[SCN]_i$ and $[Cl]_i$ (intracellular concentrations) are 150 and 4 mM, respectively; $[Cl]_o$ (extracellular) is 154 mM; and *R*, *T* and *F* have their usual thermodynamic meanings.

Experiments were carried out at room temperature, 21–24°C. Values are presented as mean ± SEM. Tests of significance were carried out using Student's two-tailed *t*-test.

Results

Identification of Pore-Lining Residues Using Macroscopic Current Recording

We used site-directed mutagenesis to introduce cysteines for each of 21 continuous residues in the outer parts of TMs 11 and 12 and in the extracellular loop connecting these two TMs (Fig. 1). The functional effects of mutations in the more central part of TM12 have previously been studied (Vankeerberghen et al. 1998; Gupta et al. 2001) and do not support a major role for this part of the protein in controlling pore properties. All 21 cysteine mutants generated large currents when expressed in BHK cells that were, like wild-type CFTR, activated by cytoplasmic PKA and ATP and further stimulated by PPi.

To identify residues that lie within the permeation pathway, we modified introduced cysteines by charged MTS reagents in the extracellular solution. As shown previously (Fatehi and Linsdell 2008), inclusion of positively charged MTSET or negatively charged MTSES in

the pipette solution did not alter the shape of the macroscopic *I–V* relationship of wild-type CFTR channels in inside–out membrane patches treated with PPi (Fig. 2a, b). This is consistent with the lack of reactivity of wild-type CFTR with external MTS reagents reported by other groups (Cheung and Akabas 1996; Smith et al. 2001; Beck et al. 2008). Similarly, no change in *I–V* shape was observed with either MTSET or MTSES in the pipette solution for 14 out of 21 cysteine mutants studied. In contrast, seven mutants were sensitive to external MTS reagents (Fig. 2). An example is S1118C (Fig. 2c, d). This mutant exhibited a macroscopic *I–V* relationship that was slightly inwardly rectified under control conditions. This rectification became less pronounced when MTSET was included in the pipette solution and even stronger with MTSES (Fig. 2c, d). These MTS-induced changes in *I–V* shape are consistent with deposition of charge in the pore by covalent modification of the introduced cysteine and consequent changes in the electrostatic attraction of Cl^- ions into the pore from the extracellular solution (Smith et al. 2001; Fatehi and Linsdell 2008; Zhou et al. 2008).

The effects of extracellular charged MTS reagents on *I–V* shape in different channel variants can be observed from relative current-voltage (I_{REL}–V) relationships such as those shown in Fig. 2e. As described previously for modification of cysteines introduced into TM6 (Fatehi and Linsdell 2008) and the extracellular loop between TMs 1 and 2 (Zhou et al. 2008), MTSET and MTSES altered the I_{REL}–V shape in S1118C, T1121C, T1122C, G1127C, V1129C, I1131C and I1132C.

Of 21 cysteine mutants studied, only six significantly altered *I–V* relationship shape in the absence of external MTS reagents (Fig. 3a), with S1118C, T1121C, T1122C, G1127C and A1136C all causing significant inward rectification and V1129C showing outward rectification. These changes in *I–V* shape following neutral amino acid substitutions appear to reflect changes in single-channel current amplitudes (see below).

The effects of charged MTS reagents on *I–V* relationship shape in all 21 mutants are summarized in Fig. 3b. As described above (Fig. 2), six mutants had *I–V* relationships that were sensitive to both MTSET and MTSES and only one (I1131C) was altered by MTSET but not MTSES. There was strong overlap between changes in control *I–V* shape and sensitivity to MTS reagents—only A1136C showed an *I–V* relationship that was significantly different in shape from wild-type in the absence of MTS reagents (Fig. 3a) but insensitive to charged MTS reagents (Fig. 3b). The dependence of *I–V* relationship shape on the predicted charge of the modified amino acid side chain for each of the seven MTS-sensitive mutants is summarized in Fig. 3c. As with cysteines introduced into other regions (Fatehi and Linsdell 2008; Zhou et al. 2008), the relationship between *I–V* shape and predicted side chain charge is consistent with effects on the electrostatic attraction of extracellular Cl^- ions into the pore.

Effects of Cysteine Mutations on Single-Channel Conductance

The charge-dependent effects of MTS modification of cysteine mutant forms of CFTR shown in Fig. 3c imply that each of these amino acid side chains lies within or close to the Cl^- permeation pathway, such that charge deposition at these positions by water-soluble reagents is able to modify Cl^- movement in the pore directly. To investigate the role of these residues in Cl^- permeation, we measured unitary Cl^- currents in each of these seven cysteine mutants (Fig. 4). Five of these mutants significantly altered the single-channel current–voltage (*i-V*) relationship (Fig. 4b)—these five mutants also altered macroscopic *I–V* relationship shape in the absence of MTS reagents (Fig. 3a). In contrast, I1131C and I1132C did not significantly affect the form of either the *i-V* relationship (Fig. 4b) or the *I–V* relationship (Fig. 3a). Only one mutant—V1129C—significantly affected the magnitude of unitary currents at hyperpolarized voltages (Figs. 4, 5a), giving a decrease in unitary current amplitude of ~12% at –80 m*V* (Fig. 5a). Unitary currents at depolarized voltages were significantly decreased in S1118C, T1121C, T1122C and G1127C and significantly increased in V1129C (Fig. 5b). This resulted in changes in the shape of the *i–V* relationship, causing inward rectification in the case of S1118C, T1121C, T1122C and G1127C and outward rectification in the case of V1129C (Figs. 4b, 5c). No changes in *i–V* shape were observed for I1131C or I1132C. All of these effects on the *i–V* relationship are in concurrence with those observed at the macroscopic current level (see Fig. 3a). Since all of these mutations involved substitution of neutral amino acid side chains with cysteine, which may carry at most a partial negative charge at neutral pH, these mutation-induced changes in single-channel currents presumably reflect nonelectrostatic effects that reflect, e.g., changes in the size or hydrophobicity of pore-lining side chains that interact with permeating Cl^- ions. It is also possible that these effects reflect more global structural changes, even though the mutated residues do appear to be pore-lining.

Effects of MTS Reagents on Single-Channel Conductance

The effects of charged MTS reagents on macroscopic *I–V* relationship shape in reactive cysteine mutants (Figs. 2 and 3) imply that these reagents alter the unitary Cl^- current amplitude in these channels, especially at depolarized voltages. Indeed, changes in unitary current amplitude were

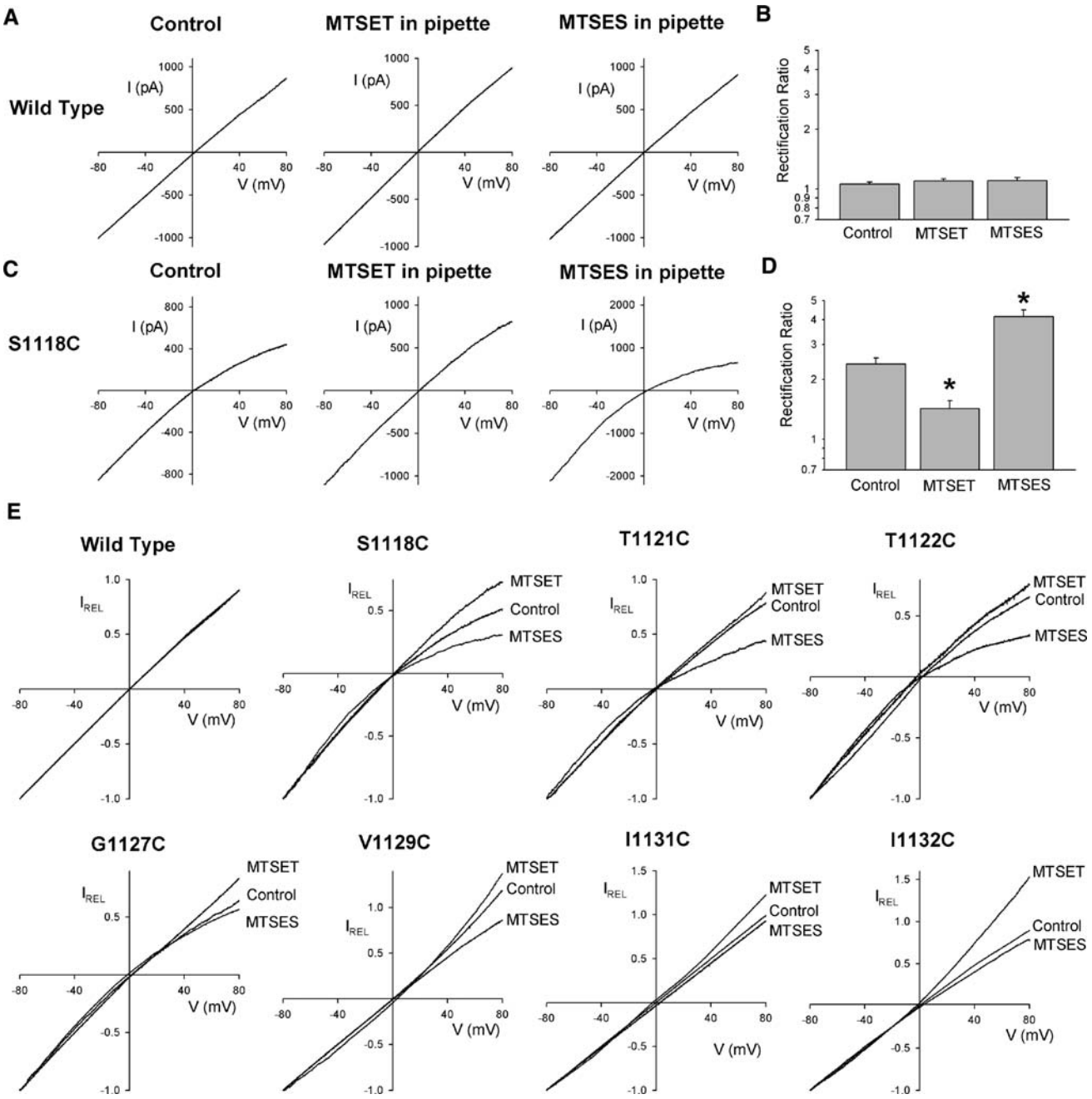

Fig. 2 Modification of cysteine mutant forms of CFTR by extracellular MTS reagents. **a** Example leak-subtracted macroscopic *I–V* relationships for wild-type CFTR. As with all macroscopic currents used in the present study, currents were recorded from inside–out membrane patches following maximal current stimulation with PKA, ATP and PPi. Currents were recorded from different membrane patches with no MTS reagent, 5 mM MTSET or 5 mM MTSES present in the extracellular (pipette) solution as indicated. **b** Mean rectification ratio estimated under these conditions. **c**, **d** Example *I–V* relationships and mean rectification ratios for S1118C under the same conditions. **e** Example I_{REL}–*V* relationships for different channel variants under control conditions and with MTSET or MTSES present in the pipette solution. Currents are plotted relative to current at –80 m*V*, as described in "Materials and Methods." Note that three separate I_{REL}–*V* relationships overlie for wild-type. **b** and **d** represent mean of data from six to nine patches. * Significant difference from control ($P < 0.001$)

observed in S1118C, T1121C, T1122C, G1127C, V1129C, I1131C and I1132C, but not wild-type, when MTS reagents were included in the pipette solution (Fig. 6). The effects of these MTS reagents on the unitary *i–V* relationships of different channel variants are shown in Fig. 7. These reagents had no effect on unitary currents in wild-type at any voltage. In those cysteine mutants studied, neither MTSET nor MTSES significantly altered unitary current amplitude at

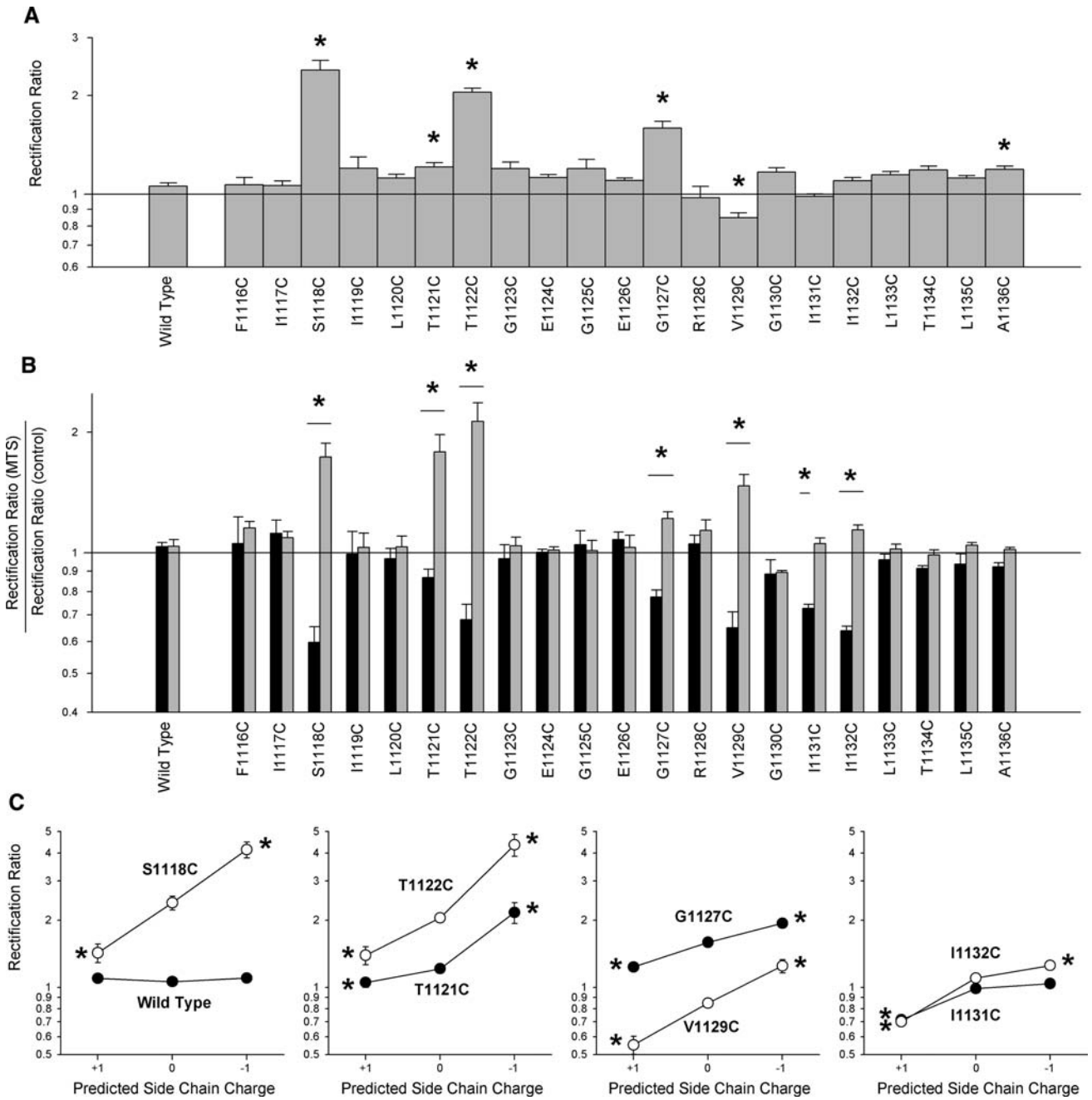

Fig. 3 Effects of external MTS reagents on macroscopic *I–V* relationship shape. **a** Mean rectification ratio for wild-type and each of the 21 cysteine mutants used in the present study, under control conditions. Mean of data from three to 10 patches. * Significant difference from wild-type ($P < 0.05$). **b** Effect of external MTSET (*black bars*) and MTSES (*gray bars*) on the rectification ratio in each channel variant. **c** Mean rectification ratios estimated with or without charged MTS reagents present in the pipette solution, plotted as a function of predicted side chain charge following modification (+1 with MTSET, 0 control, –1 with MTSES). It is presumed that no modification takes place in wild-type, and here predicted charge represents the charge of the modifying reagent present. The side chain charge of the introduced cysteine may not in fact be zero but slightly negative (Smith et al. 2001); furthermore, it is possible that the extent of the partial negative charge may be different at different sites. **b** and **c** represent means of data from three to nine patches. * Significant difference from control (no MTS reagent) for the same channel variant ($P < 0.05$). Note that the rectification ratio in six cysteine mutants is significantly affected by both MTSET and MTSES (indicated by *asterisks*), whereas in a seventh (I1131C) it is significantly altered by MTSET but not by MTSES

hyperpolarized potentials; however, in most cases unitary current amplitude at depolarized voltages was increased by MTSET and decreased by MTSES. These specific, voltage-dependent changes in unitary current amplitude resulted in changes in *i–V* relationship shape (Fig. 7). Using the ratio of unitary current amplitude at hyperpolarized and depolarized

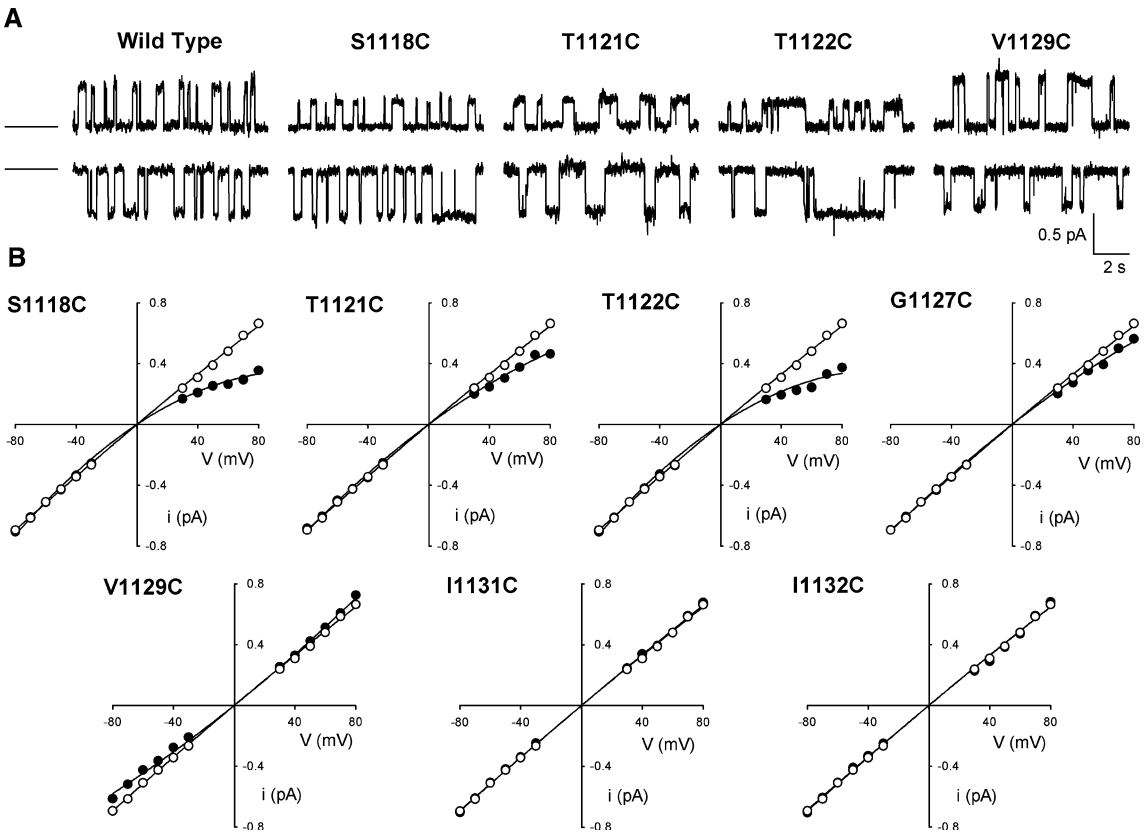

Fig. 4 Single-channel currents carried by cysteine mutant forms of CFTR. **a** Example single-channel currents carried by wild-type, S1118C, T1121C, T1122C and V1129C, at membrane potentials of +60 (*top*) and –60 (*bottom*) m*V*. The *line to the left* represents the closed channel current level. **b** Mean single-channel *i–V* relationships. In each panel *open circles* represent wild-type and *filled circles,* the cysteine mutant named on the plot. Mean of data from three to seven patches

voltages as an indicator, Fig. 8 shows that MTS reagents had charge-dependent effects on *i–V* relationship shape that broadly mirrored those observed in the macroscopic *I–V* relationships (see Fig. 3c). Thus, it appears that the effects of charged MTS reagents on macroscopic *I–V* relationship shape in cysteine mutant forms of CFTR reflect predominantly changes in unitary current amplitude at depolarized voltages.

Significant effects of MTS modification on unitary current amplitude were observed only at depolarized voltages, reflecting effects on Cl^- entry from the extracellular solution. Considering the effect of modifying the charge at different positions by mutation and MTS modification on unitary current amplitude at +80 m*V*, there appear to be two distinct, site-dependent effects. Four mutations (S1118C, T1121C, T1122C, G1127C) led to significant decreases in unitary current amplitude (Fig. 5b), which were relatively strongly affected by MTS modification—in each case conductance was further decreased by reaction with MTSES and increased to near wild-type levels by MTSET (Fig. 9a). In contrast, the other three mutations (V1129C, I1131C, I1132C) led to no change or even a slight increase in unitary current amplitude (Fig. 5b) and more minor effects of MTS modification, resulting in no change or a small decrease in amplitude with MTSES and increases in amplitude to levels above wild-type with MTSET (Fig. 9b).

Other Functional Effects of Cysteine Mutations

Since several substituted cysteines appear to be within the permeation pathway, we considered whether these mutations would affect other functional properties of the pore, such as anion binding or anion selectivity. Block of Cl^- permeation by the permeant SCN^- anion, which has a relatively high affinity for the pore, was used as a probe of anion binding inside the pore (Gupta et al. 2001; Linsdell 2001a). As shown in Fig. 10, addition of 10 mM SCN^- to the intracellular solution led to voltage-dependent block of macroscopic Cl^- currents in wild-type CFTR, following channel treatment with PPi. This result is consistent with the effects of SCN^- on unitary current amplitude (Linsdell 2001b; Fatehi et al. 2007). Under these conditions, SCN^- block was significantly strengthened in I1132C (at hyperpolarized and depolarized voltages), S1118C (at hyperpolarized voltages), T1121C and V1129C (at depolarized voltages) and I1131C (at very depolarized voltages only)

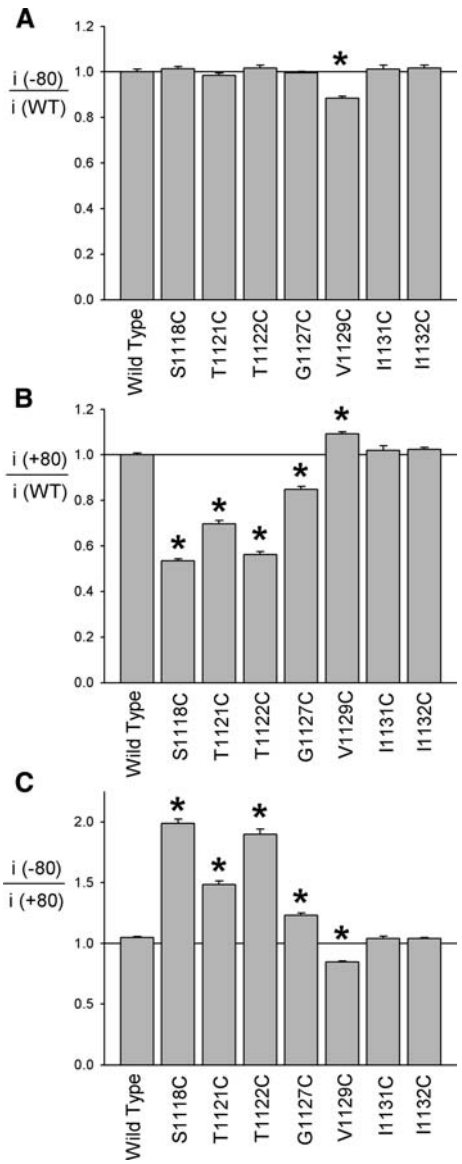

Fig. 5 Effect of cysteine mutations on single-channel current amplitude. **a**, **b** Single-channel current amplitude at –80 (**a**) and +80 (**b**) m*V* as a fraction of the corresponding mean value in wild-type. **c** Ratio of unitary current amplitudes at –80 and +80 m*V*, a measure of the degree of rectification of the *i–V* relationship. Mean of data from three to six patches in each panel. * Significant difference from wild-type ($P < 0.05$)

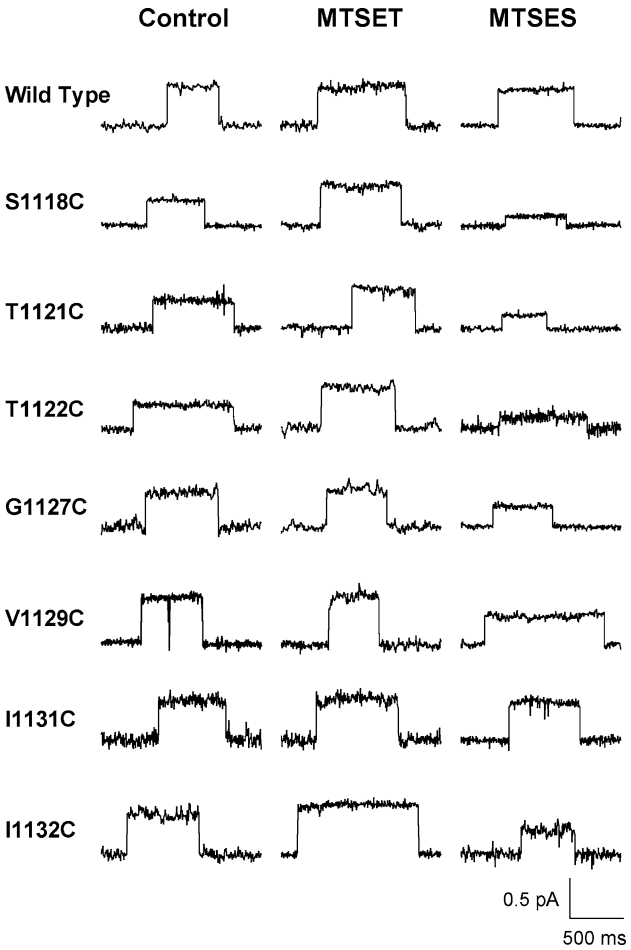

Fig. 6 Effect of MTS reagents on single-channel currents. Example single-channel currents recorded at +60 m*V* for different channel variants as described on the *left*, without MTS reagents (Control) or with 5 mM MTSET or MTSES present in the extracellular (pipette) solution. Channel openings are reflected by upward deflections of the current trace (compare with Fig. 4a)

(Fig. 10). Block was not significantly altered in either T1122C or G1127C (data not shown). In no case was SCN^- block significantly weakened, which might suggest disruption of an anion-binding site in the pore as a result of mutation.

Alteration of CFTR anion selectivity was determined by estimating SCN^- permeability, using macroscopic current reversal potential measurements with SCN^--containing bath solutions (Ge et al. 2004). Under these conditions, SCN^- permeability was significantly increased in S1118C and (to a lesser extent) T1122C and G1127C and unaltered in T1121C, V1129C, I1131C and I1132C (Fig. 11).

Discussion

Functional Modification of Introduced Cysteines as a Screen for Pore-Lining Residues

The SCAM technique identifies amino acid side chains that are accessible to water-soluble reagents, suggesting that they are present at some interface between the protein and the solvent. On the other hand, analysis of the functional effects of mutations on channel permeation properties such as single-channel conductance, intrapore ion binding and ion selectivity pinpoints functionally important amino acids but does not necessarily provide information on side

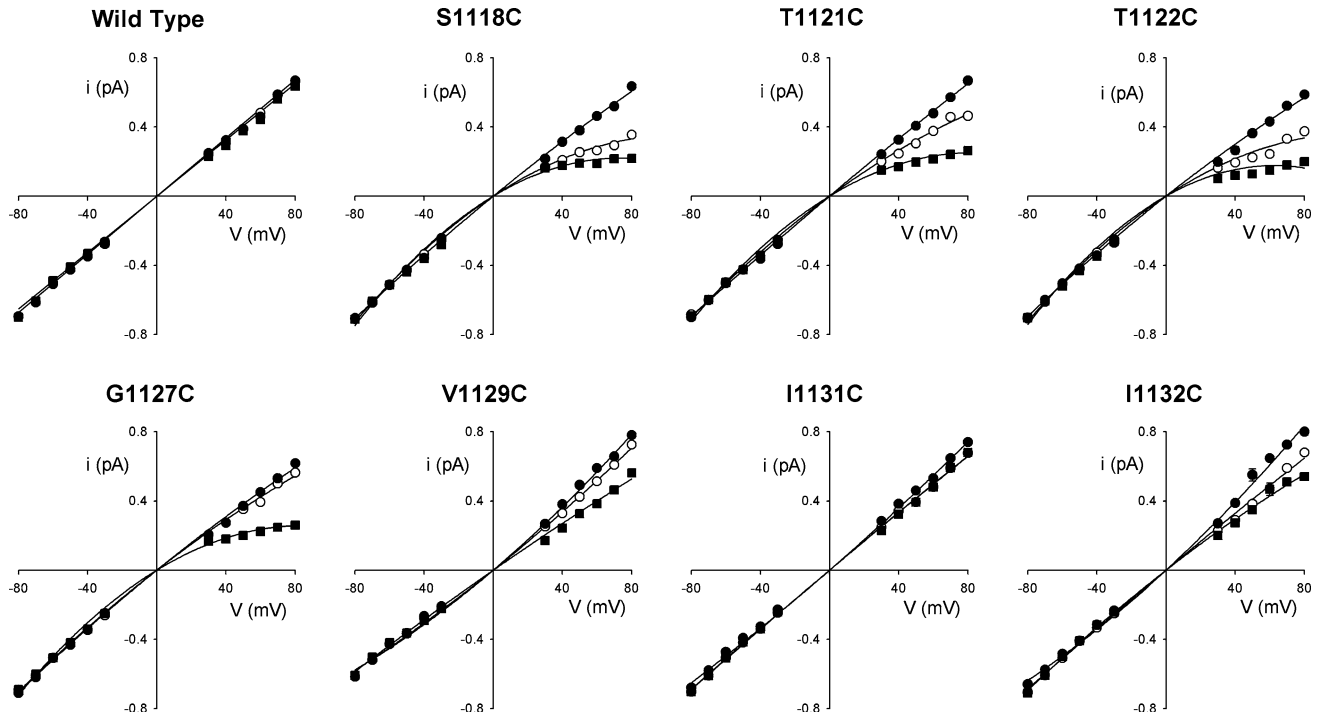

Fig. 7 Effect of MTS reagents on unitary *i–V* relationships. Mean single-channel *i–V* relationships for the named channel variants, recorded in the absence of MTS reagents (○) or with 5 mM MTSET (●) or MTSES (■) present in the extracellular solution. Mean of data from three to seven patches

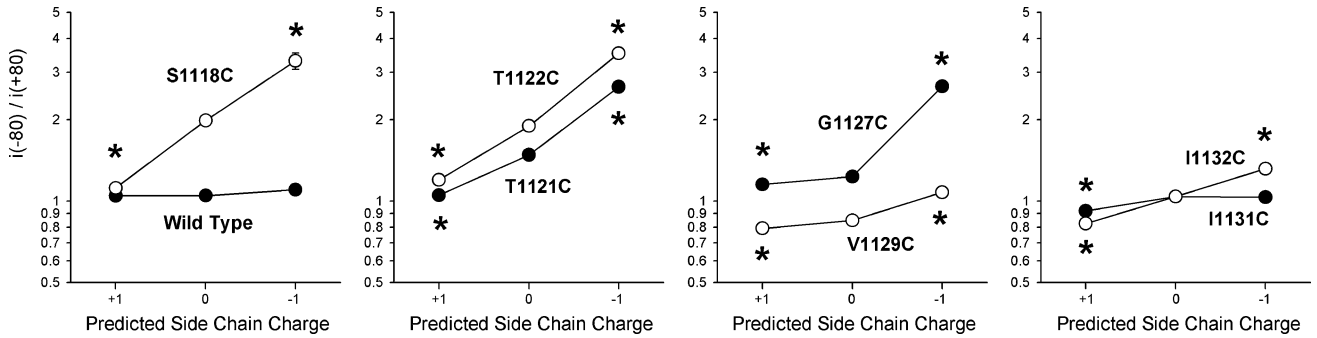

Fig. 8 Modification by charged MTS reagents alters the shape of the *i–V* relationship in cysteine mutants. The ratio of unitary current amplitudes at –80 and +80 m*V*, used as a measure of the degree of rectification of the *i–V* relationship (see Fig. 5c), is plotted as a function of predicted side chain charge following modification (+1 with MTSET, 0 control, –1 with MTSES). Mean of data from three to five patches. * Significant difference from control (no MTS reagent) for the same channel variant ($P < 0.05$)

chain accessibility. Our approach here was to combine SCAM with a functional measurement that directly reports pore function in order to identify amino acid side chains that are exposed within the ion permeation pathway. Screening cysteine substituted mutants for MTS reagent–induced changes in *I–V* shape afforded us a simple method to identify amino acid side chains that lie within the permeation pathway of CFTR. The shape of the *I–V* relationship is an easily identified parameter that is quite invariant between different patches (especially following treatment with PPi to minimize the influence of channel gating) and independent of current amplitude and, furthermore, is expected to directly reflect MTS-dependent changes in channel permeation properties but to be insensitive to MTS-induced changes in channel gating (see below).

Using this approach, we found that seven of 21 continuous residues in the TM11–extracellular loop–TM12 region were functionally modified by external MTS reagents (Fig. 3b). This includes two residues (I1131 and I1132) for which mutation to cysteine had no effect on single-channel conductance in the absence of MTS reagents (Figs. 4b, 5). In all seven cases, positively charged MTSET caused changes in the shape of the *I–V*

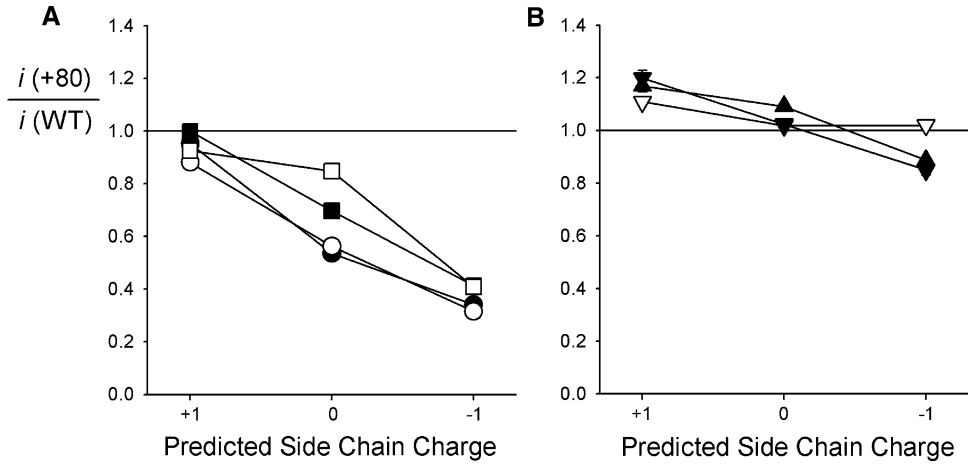

Fig. 9 Effects of MTS modification on unitary current amplitude at depolarized voltages. Both panels show unitary current amplitude at +80 m*V* as a fraction of mean amplitude in wild-type under the same conditions, plotted as a function of predicted side chain charge following MTS modification (+1 with MTSET, 0 control, −1 with MTSES). **a** S1118C (●), T1121C (■), T1122C (◯), G1127C (□); **b** V1129C (▲), I1131C (▽), I1132C (▼). Mean of data from three to five patches

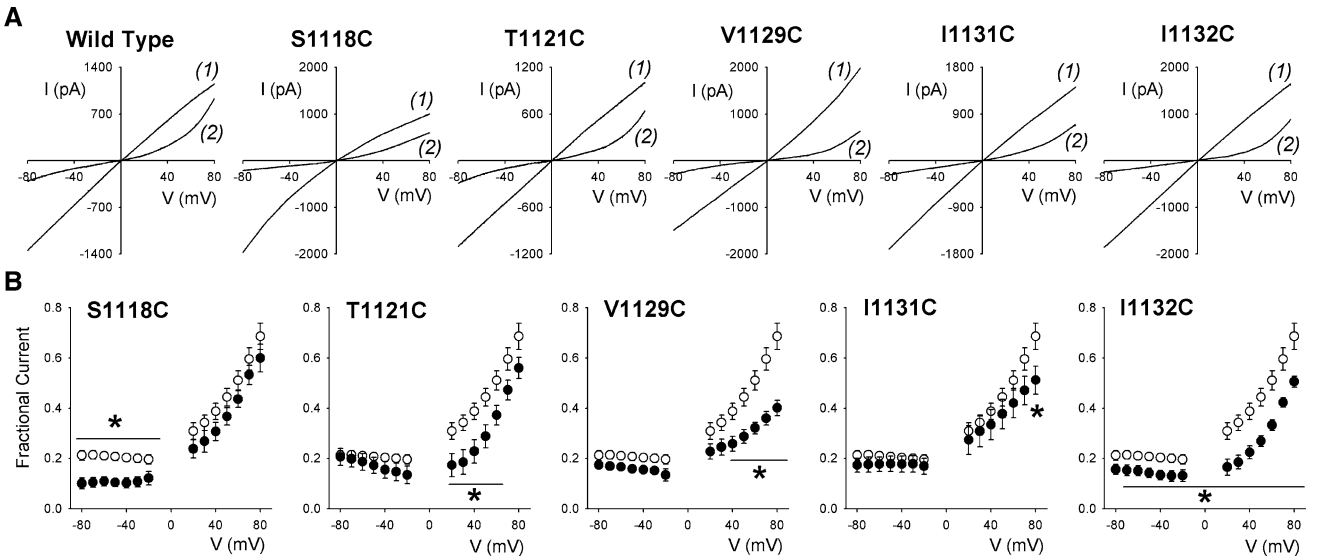

Fig. 10 Thiocyanate block of cysteine mutants. **a** Example leak-subtracted macroscopic *I–V* relationships for the different CFTR variants named, following maximal channel activation with ATP, PKA and PPi. In each case, currents were recorded before (*1*) and following (*2*) addition of 10 mM SCN^- to the intracellular (bath) solution. **b** Mean fractional current remaining following addition of SCN^- as a function of voltage. In each panel *open circles* represent wild-type and *filled circles*, the named cysteine mutant. *Asterisks* indicate the voltage ranges over which the blocking effects of SCN^- were significantly altered in each mutant compared to wild-type ($P < 0.05$)

relationship (Figs. 2e, 3b, 3c) that appeared to be due to selective increases in unitary current amplitude at depolarized voltages (Figs. 7, 9). This is consistent with the hypothesis that covalent modification with MTSET increases the electrostatic attraction of Cl^- ions into the pore from the extracellular solution, increasing the amplitude of currents carried by Cl^- influx. Conversely, in six out of seven cases, negatively charged MTSES had a quantitatively opposite effect on *I–V* relationship shape (Figs. 2e, 3b, c) that appeared to be due to selective decreases in unitary current amplitude at depolarized voltages (Figs. 7, 9). This effect of MTSES is consistent with reduced overall attraction of extracellular Cl^- ions into the pore. Overall the effects of MTS reagents at the macroscopic and single-channel levels were quite consistent (e.g., compare Figs. 3c and 8), although minor quantitative discrepancies may result from the ways in which effects on different currents were analyzed and quantified. This broad agreement between effects observed at the macroscopic and single-channel levels confirms that the changes in *I–V* relationship shape predominantly reflect changes in the permeation properties of the channel, suggesting that this approach is an effective screen of pore-lining side chains.

Of the seven mutants that were functionally modified by MTS reagents, five (S1118C, T1121C, T1122C, G1127C, V1129C) also showed significantly altered unitary current amplitude in the absence of MTS modification (Figs. 4, 5).

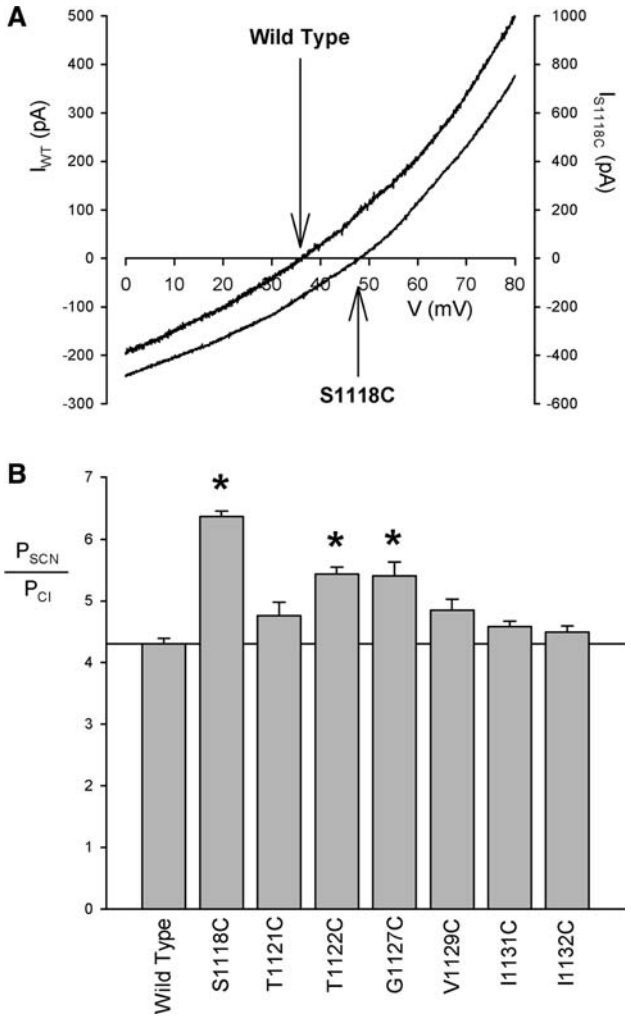

Fig. 11 Thiocyanate permeability of mutants. **a** Example leak-subtracted *I–V* relationships recorded with Cl^--containing extracellular solutions and SCN^--containing intracellular solutions. In these examples, the current reversal potential is +36.4 m*V* for wild-type and +47.8 m*V* for S1118C (shown by *arrows*), suggesting an increased P_{SCN}/P_{Cl} in this mutant. **b** Mean P_{SCN}/P_{Cl} values calculated from reversal potential measurements under these conditions as described in "Materials and Methods." Mean of data from four to six patches. * Significant difference from wild-type ($P < 0.05$)

Since these changes resulted from substitution of neutral amino acid side chains by cysteine, we assume that, unlike the charge-sensitive effects of MTS modification described above, they reflect nonelectrostatic effects on interactions with permeating Cl^- ions. Neutral mutations in the central region of TM6, at F337 (Linsdell 2001a), T338 (Linsdell et al. 1998) and S341 (McDonough et al. 1994), also reduce single-channel conductance, especially at depolarized voltages. Only one mutant that was apparently not affected by MTS reagents (A1136C) had a small effect on the shape of the *I–V* relationship (Fig. 3a). This may reflect an indirect effect of mutating a non-pore-lining residue (A1136) that results in a small change in open channel current amplitude. However, we cannot rule out the possibility that the side chain at this position is pore-lining but for some reason inaccessible to extracellular MTS reagents. Mutations at all other sites did not affect either *I–V* relationship shape or sensitivity to MTS reagents. We suggest that these most likely reflect nonaccessible amino acid side chains, although as with all cysteine modification experiments it is possible that modification did take place but was without functional consequence by our assays. Since modification at so many sites appears to have a qualitatively similar, charge-dependent effect on Cl^- permeation—even in cases where mutation to cysteine itself had no apparent effect—we believe the likelihood of such "false negatives" is low.

The functional modification of introduced cysteines approach we describe is sensitive to MTS-induced changes in channel permeation properties but would be insensitive to MTS-induced changes in channel gating. First, our macroscopic current experiments use PPi to prevent channel closure, such that the rate of channel gating is expected to be very slow relative to the duration of the voltage ramps used. Second, since different membrane patches are used for control and MTS-modified channels, differences in overall current levels cannot be compared to give any information on relative levels of channel activity. Effects of external MTS reagents on the gating of CFTR cysteine mutants (I331C, L333C) have been described (Beck et al. 2008) but would presumably not be noticed using our experimental approach. Effects on channel gating could reflect modification of pore-lining or non-pore-lining side chains and, thus, are a less good screen of the pore than the effects on electrostatic interactions with Cl^- ions that we describe. In other words, we have intentionally designed our experiments (unlike more conventional SCAM approaches) to be sensitive to effects on permeation and not gating in order to identify residues that lie within the permeation pathway.

Functional Effects of Charge Deposition in the Pore

Since MTS modification of introduced cysteines appears to affect primarily Cl^- entry from the extracellular solution, we consider that all mutations studied are in the mid- to outer region of the CFTR pore. This location is consistent with the expected location of the mutated residues in the outer parts of TMs 11 and 12 and the extracellular loop that joins these TMs (Fig. 1). The effects of MTS modification of introduced cysteines, and of the mutations themselves, on unitary current amplitudes appear to reflect one of two distinct patterns depending on the location of the reactive side chain (Fig. 9). We speculate that one group of reactive mutants (S1118C, T1121C, T1122C, G1127C) is located relatively deep in the pore from the outside and that the other (V1129C,

I1131C, I1132C) represents mutations at the outermost mouth of the pore. In this scenario, charge-neutral mutations deeper in the pore (S1118C, T1121C, T1122C, G1127C) (Fig. 9a) disrupt Cl^- movement in the pore in a nonelectrostatic fashion, leading to reduced unitary currents at depolarized voltages, as described previously for TM6 mutations (McDonough et al. 1994; Linsdell et al. 1998; Linsdell 2001a). These mutants were also, for the most part, strongly sensitive to modification by both MTSET and MTSES. Reductions in conductance were partially counteracted by introducing an attractive positive charge by MTSET modification, although in no case was this able to restore conductance completely to wild-type values, consistent with some important interaction between Cl^- ions and the pore having been disrupted by the mutation. Chloride conductance was further reduced by MTSES modification at these sites, indicating the detrimental effect of depositing a negative charge within the permeation pathway. Cysteine substitution at the outer mouth of the pore (V1129C, I1131C, I1132C) (Fig. 9b) had somewhat different effects. These mutations had only small effects on Cl^- conductance. Furthermore, the overall effects of MTS modification here appear to be smaller. Addition of positive or negative charge to these sites by MTS modification may alter the distribution of surface charges around the pore entrance, either increasing or decreasing the availability of Cl^- ions to enter the pore from the outside and subtly altering unitary conductance. In the case of modification by positively charged MTSET, the proposed increase in overall surface charge leads to a significant increase in unitary conductance over wild-type levels (Fig. 9b). MTSES modification in this region has only very minor effects, perhaps due to the presence of local endogenous positive charges (Zhou et al. 2008). While other factors, such as the location of endogenous fixed charges, the location and occupancy of Cl^- ion binding sites and differences in accessibility, may also contribute to the relative effect of MTS modification at different sites, the scenario described above appears to be consistent with the proposed locations of the modified side chains (Fig. 1). Thus, it appears that pore-lining side chains throughout the outer part of the CFTR pore can be positively identified using the functional modification of substituted cysteines approach we outline.

Roles of TM11 and TM12 in Formation of the Pore

The above scenario suggests that TM11 residues S1118, T1121, T1122 and G1127 are located relatively deep in the pore from its extracellular end, with V1129, I1131 and I1132 in the extracellular loop between TM11 and TM12 being at the outermost part of the pore (Fig. 1). Mutations S1118C, T1122C and G1127C also altered the anion selectivity of CFTR, significantly increasing SCN^- permeability (Fig. 11), which is consistent with changes in pore structure and function. Previously, SCN^- permeability was shown to be significantly decreased in S1118F but unaltered in S1118A (Zhang et al. 2000). Anion selectivity is most highly sensitive to mutations in similar regions of TM6 (F337, T338) and TM1 (A96) (Linsdell et al. 2000; Ge et al. 2004).

Several cysteine mutations also affected SCN^- block of Cl^- permeation (Fig. 10). These effects could reflect altered interactions between SCN^- ions and the pore, altered interactions between SCN^- and Cl^- ions in the pore or altered movement of SCN^- ions between different sites inside the pore (Fatehi et al. 2007). Since the changes illustrated in Fig. 10 were considered to be relatively minor gain-of-function effects, their origins were not investigated in further detail. Mutations throughout TMs 1–6 significantly strengthen block by the lyotropic permeant anion $Au(CN)_2^-$ by unknown mechanisms (Ge et al. 2004), suggesting this is not a specific effect but instead reflects that anion binding is highly sensitive to mutations within the TMs. In contrast to the minor effects illustrated in Fig. 10, major disruption of $Au(CN)_2^-$ block is observed following mutation of K95 in TM1 (Ge et al. 2004) and R334 in TM6 (Gong and Linsdell 2003b). We consider it unlikely that any of the residues mutated in the present study make an important contribution to a permeant anion-binding site in the pore that is involved in SCN^- block. Nevertheless, these residues do appear to have some impact on the interaction of permeant anions with the pore.

The structure of the TM11–extracellular loop–TM12 region of CFTR is not known; however, molecular modeling has suggested that these TMs are α-helical in structure and connected by a short extracellular linker (Mornon et al. 2008; Serohijos et al. 2008). Our functional results suggesting that residues throughout this region are close to the outer mouth of the permeation pathway appear to be in broad agreement with these models.

Interestingly, the region we selected for mutagenesis (Fig. 1) includes three amino acids with charged side chains—E1124, E1126 and R1128—yet none of these charged side chains appears to contribute to the permeation pathway (Fig. 3). These charged residues may play other roles, such as stabilization of protein structure.

It should be stressed that, in some cases, the cysteine mutations we used in the present study represent rather conservative mutations (especially S1118C, which effectively changes one oxygen atom to sulfur). The present results should, by identifying amino acid side chains located in the permeation pathway, be viewed as a starting point for future structure–function analyses of this region.

Implications for the Structure and Function of the CFTR Channel Pore

Our results suggest that TM11 contributes to the CFTR channel pore and influences Cl^- movement into the pore from the extracellular solution. To put these results into context, our group reported similar subtle changes in single-channel conductance, permeant anion binding and SCN^- permeability following mutation of the analogous part of TM5 (Ge et al. 2004), although the accessibility of TM5 side chains has not been reported. Mutations in the same outer part of TM1 and TM6 have a much greater impact on each of these aspects of pore function (Ge et al. 2004), and these TMs may play dominant roles in determining the permeation properties of CFTR (Linsdell 2006). Furthermore, TMs 1 and 6 have previously been shown by SCAM to line the pore (Akabas et al. 1994; Cheung and Akabas 1996; Beck et al. 2008). We propose that the outer region of the CFTR pore is formed by TMs 1, 5, 6 and 11. Other TMs may contribute to the pore inner vestibule (McDonough et al. 1994; St. Aubin et al. 2007).

Acknowledgements We thank Elizabeth VandenBerg and Julie Comeau for technical assistance. We also thank Dr. Elizabeth Cowley for comments on the manuscript. This work was supported by the Canadian Institutes of Health Research.

References

Akabas MH (1998) Channel-lining residues in the M3 membrane-spanning segment of the cystic fibrosis transmembrane conductance regulator. Biochemistry 37:12233–12240

Akabas MH, Kaufmann C, Cook TA, Archdeacon P (1994) Amino acid residues lining the chloride channel of the cystic fibrosis transmembrane conductance regulator. J Biol Chem 269:14865–14868

Beck EJ, Yang Y, Yaemsiri S, Raghuram V (2008) Conformational changes in a pore-lining helix coupled to CFTR channel gating. J Biol Chem 283:4957–4966

Chang X-B, Kartner N, Seibert FS, Aleksandrov AA, Kloser AW, Kiser GL, Riordan JR (1998) Heterologous expression systems for study of cystic fibrosis transmembrane conductance regulator. Methods Enzymol 292:616–629

Cheung M, Akabas MH (1996) Identification of cystic fibrosis transmembrane conductance regulator channel-lining residues in and flanking the M6 membrane-spanning segment. Biophys J 70:2688–2695

Dawson RJP, Locher KP (2006) Structure of a bacterial multidrug ABC transporter. Nature 443:180–185

Fatehi M, Linsdell P (2008) State-dependent access of anions to the cystic fibrosis transmembrane conductance regulator chloride channel pore. J Biol Chem 283:6102–6109

Fatehi M, St. Aubin CN, Linsdell P (2007) On the origin of asymmetric interactions between permeant anions and the CFTR chloride channel pore. Biophys J 92:1241–1253

Gadsby DC, Vergani P, Csanády L (2006) The ABC protein turned chloride channel whose failure causes cystic fibrosis. Nature 440:477–483

Ge N, Muise CN, Gong X, Linsdell P (2004) Direct comparison of the functional roles played by different transmembrane regions in the cystic fibrosis transmembrane conductance regulator chloride channel pore. J Biol Chem 279:55283–55289

Gong X, Burbridge SM, Cowley EA, Linsdell P (2002) Molecular determinants of Au(CN)2-binding and permeability within the cystic fibrosis transmembrane conductance regulator Cl-channel pore. J Physiol 540:39–47

Gong X, Linsdell P (2003a) Mutation-induced blocker permeability and multi-ion block of the CFTR chloride channel pore. J Gen Physiol 122:673–687

Gong X, Linsdell P (2003b) Molecular determinants and role of an anion binding site in the external mouth of the CFTR chloride channel pore. J Physiol 549:387–397

Gupta J, Evagelidis A, Hanrahan JW, Linsdell P (2001) Asymmetric structure of the cystic fibrosis transmembrane conductance regulator chloride channel pore suggested by mutagenesis of the twelfth transmembrane region. Biochemistry 40:6620–6627

Karlin A, Akabas MH (1998) Substituted-cysteine accessibility method. Methods Enzymol 293:123–144

Kidd JF, Kogan I, Bear CE (2004) Molecular basis for the chloride channel activity of cystic fibrosis transmembrane conductance regulator and the consequences of disease-causing mutations. Curr Top Dev Biol 60:215–249

Linsdell P (2001a) Relationship between anion binding and anion permeability revealed by mutagenesis within the cystic fibrosis transmembrane conductance regulator chloride channel pore. J Physiol 531:51–66

Linsdell P (2001b) Thiocyanate as a probe of the cystic fibrosis transmembrane conductance regulator chloride channel pore. Can J Physiol Pharmacol 79:573–579

Linsdell P (2005) Location of a common inhibitor binding site in the cytoplasmic vestibule of the cystic fibrosis transmembrane conductance regulator chloride channel pore. J Biol Chem 280:8945–8950

Linsdell P (2006) Mechanism of chloride permeation in the cystic fibrosis transmembrane conductance regulator chloride channel. Exp Physiol 91:123–129

Linsdell P, Evagelidis A, Hanrahan JW (2000) Molecular determinants of anion selectivity in the cystic fibrosis transmembrane conductance regulator chloride channel pore. Biophys J 78:2973–2982

Linsdell P, Gong X (2002) Multiple inhibitory effects of $Au(CN)_2^-$ ions on cystic fibrosis transmembrane conductance regulator Cl^- channel currents. J Physiol 540:29–38

Linsdell P, Hanrahan JW (1996) Disulphonic stilbene block of cystic fibrosis transmembrane conductance regulator Cl^- channels expressed in a mammalian cell line and its regulation by a critical pore residue. J Physiol 496:687–693

Linsdell P, Hanrahan JW (1998) Adenosine triphosphate-dependent asymmetry of anion permeation in the cystic fibrosis transmembrane conductance regulator chloride channel. J Gen Physiol 111:601–614

Linsdell P, Zheng S-X, Hanrahan JW (1998) Non-pore lining amino acid side chains influence anion selectivity of the human CFTR Cl^- channel expressed in mammalian cell lines. J Physiol 512:1–16

Linton KJ (2007) Structure and function of ABC transporters. Physiology 22:122–130

McCarty NA (2000) Permeation through the CFTR chloride channel. J Exp Biol 203:1947–1962

McCarty NA, Zhang Z-R (2001) Identification of a region of strong discrimination in the pore of CFTR. Am J Physiol 281:L852–L867

McDonough S, Davidson N, Lester HA, McCarty NA (1994) Novel pore-lining residues in CFTR that govern permeation and open-channel block. Neuron 13:623–634

Mornon J-P, Lehn P, Callebaut I (2008) Atomic model of human cystic fibrosis transmembrane conductance regulator: membrane-spanning domains and coupling interfaces. Cell Mol Life Sci 65:2594–2612

Rosenberg MF, Kamis AB, Aleksandrov LA, Ford RC, Riordan JR (2004) Purification and crystallization of the cystic fibrosis transmembrane conductance regulator (CFTR). J Biol Chem 279:39051–39057

Serohijos AWR, Hegedüs T, Aleksandrov AA, He L, Cui L, Dokholyan NV, Riordan JR (2008) Phenylalanine-508 mediates a cytoplasmic-membrane domain contact in the CFTR 3D structure crucial to assembly and channel function. Proc Natl Acad Sci USA 105:3256–3261

Sheppard DN, Rich DP, Ostedgaard LS, Gregory RJ, Smith AE, Welsh MJ (1993) Mutations in CFTR associated with mild-disease-form Cl^- channels with altered pore properties. Nature 362:160–164

Smith SS, Liu X, Zhang Z-R, Sun F, Kriewall TE, McCarty NA, Dawson DC (2001) CFTR: covalent and noncovalent modification suggests a role for fixed charges in anion conduction. J Gen Physiol 118:407–431

St. Aubin CN, Linsdell P (2006) Positive charges at the intracellular mouth of the pore regulate anion conduction in the CFTR chloride channel. J Gen Physiol 128:535–545

St. Aubin CN, Zhou J-J, Linsdell P (2007) Identification of a second blocker binding site at the cytoplasmic mouth of the CFTR chloride channel pore. Mol Pharmacol 71:1360–1368

Vankeerberghen A, Wei L, Teng H, Jaspers M, Cassiman J-J, Nilius B, Cuppens H (1998) Characterization of mutations located in exon 18 of the *CFTR* gene. FEBS Lett 437:1–4

Zhang Z-R, McDonough SI, McCarty NA (2000) Interaction between permeation and gating in a putative pore domain mutant in the cystic fibrosis transmembrane conductance regulator. Biophys J 79:298–313

Zhou J-J, Fatehi M, Linsdell P (2007) Direct and indirect effects of mutations at the outer mouth of the cystic fibrosis transmembrane conductance regulator chloride channel pore. J Membr Biol 216:129–142

Zhou J-J, Fatehi M, Linsdell P (2008) Identification of positive charges situated at the outer mouth of the CFTR chloride channel pore. Pflügers Arch 457:351–360